Kinetics of ergodic-to-nonergodic transitions in charged colloidal suspensions: Aging and gelation

Hajime Tanaka,[1] Sara Jabbari-Farouji,[2] Jacques Meunier,[3] and Daniel Bonn[2,3]
[1]*Institute of Industrial Science, University of Tokyo, Meguro-ku, Tokyo 153-8505, Japan*
[2]*Van der Waals–Zeeman Institute, Valckenierstraat 65, 1018XE Amsterdam, the Netherlands*
[3]*Laboratoire de Physique Statistique, Ecole Normale Supérieure, 24 rue Lhomond, 75005 Paris, France*
(Received 18 May 2004; revised manuscript received 5 October 2004; published 9 February 2005)

There are two types of isotropic disordered nonergodic states in colloidal suspensions: colloidal glasses and gels. In a recent paper [H. Tanaka, J. Meunier, and D. Bonn, Phys. Rev. E **69**, 031404 (2004)], we discussed the static aspect of the differences and the similarities between the two. In this paper, we focus on the dynamic aspect. The kinetics of the liquid-glass transition is called "aging," while that of the sol-gel transition is called "gelation." The former is primarily governed by repulsive interactions between particles, while the latter is dominated by attractive interactions. Slowing down of the dynamics during aging reflects the increasing cooperativity required for the escape of a particle from the cage formed by the surrounding particles, while that during gelation reflects the increase in the size of particle clusters towards the percolation transition. Despite these clear differences in the origin of the slowing down of the kinetics between the two, it is not straightforward experimentally to distinguish them in a clear manner. For an understanding of the universal nature of ergodic-to-nonergodic transitions, it is of fundamental importance to elucidate the differences and the similarities in the kinetics between aging and gelation. We consider this problem, taking Laponite suspension as an explicit example. In particular, we focus on the two types of nonergodic states: (i) an attractive gel formed by van der Waals attractions for high ionic strengths and (ii) a repulsive Wigner glass stabilized by long-range Coulomb repulsions for low ionic strengths. We demonstrate that the aging of colloidal Wigner glass crucially differs not only from gelation, but also from the aging of structural and spin glasses. The aging of the colloidal Wigner glass is characterized by the unique cage-forming regime that does not exist in the aging of spin and structural glasses.

DOI: 10.1103/PhysRevE.71.021402 PACS number(s): 82.70.Dd, 64.75.+g, 83.10.Pp, 05.70.Fh

I. INTRODUCTION

Both colloidal gels and glasses are interesting solid (or jammed [1–3]) states of condensed matter with soft elasticity. The difference between gels and glasses is rather clear in their ideal limits. The elasticity of gels stems from an infinite percolated network [4], while that of glasses stems from caging effects [5]. In a recent paper [6], we discussed the differences and similarities between these two types of nonergodic states from the static aspect. In this paper, we focus on the kinetic aspect.

The process of liquid-glass transition is called "aging," while that of sol-gel transition is called "gelation." During aging, a system explores the energy landscape by thermally overcoming barriers in order to lower the total energy. The more the system is aged, the higher the barriers it must overcome. This is the origin of the slowing down of the kinetics during aging. Eventually, the system falls into a steep valley, from which it can no longer escape during the observation time, and thus becomes nonergodic. During gelation, on the other hand, particles form clusters whose size keeps increasing in time. Eventually, clusters form a percolated network and the system becomes nonergodic. Towards this percolation transition, the characteristic relaxation time of the system diverges, reflecting the growth of the clusters with time. Both processes can be characterized as an ergodic-to-nonergodic transition and by the resulting appearance of elasticity. Because of this, the similarity between glass and gel is much emphasized in the literature (see, e.g., Ref. [7]). However, there may also be crucial differences, reflecting the fundamental differences in the mechanism of the slowing down between the two.

We consider this fundamental problem, taking Laponite suspension as an explicit example. It is known that a suspension of charged colloidal clay particles, Laponite [8], forms a very uniform, isotropic soft solid state. Due to the competition between long-range electrostatic repulsions and van der Waals attractions, both nonergodic states, glass and gel, can form even in a very dilute suspension, where the volume fraction of Laponite ϕ is on the order of $\sim 1\%$. This is markedly different from the case of usual colloidal suspensions without charges, where the volume fraction required for glass formation is in the order of $\sim 50\%$. As discussed in our recent paper [6], for low ionic strengths, Laponite forms a colloidal Wigner glass [9–12], while for high ionic strengths it forms a colloidal gel [13–20]. This suggests that a glass-to-gel transition can occur in Laponite suspensions [6]. Because of these interesting features, the nonergodic states of Laponite suspensions have recently attracted considerable attention from both fundamental and applied viewpoints [9–20]. Since the interactions between particles are weak in such dilute suspensions, both aging and gelation take place very slowly. This provides us with a unique opportunity to study both the kinetics of aging and gelation in detail.

In relation to the ability of Laponite suspensions to form these nonergodic states even for dilute suspensions, we point out that the glassy nonergodic state of such a suspension is crucially different from that of usual glass-forming liquids such as simple liquids, oxides, and metals [5]: Laponite suspensions have elasticity but at the same time contain a fluid

as its component. The mechanical stress is asymmetrically divided between the components. The elastic part of the stress is supported by their elastic components (i.e., particles), and not by the fluid component. This means that the word "nonergodic" applies only to the elastic component, and obviously does not apply to the fluid component. The effect of this fluid component on the kinetics of the ergodic-to-nonergodic transition has not attracted much attention so far and remains to be clarified. This should be particularly important for the interesting example of aging under stress. Furthermore, colloidal suspensions often have other components such as polymers or salts, which control the interparticle interactions. Effects of these multicomponent features may also significantly affect the dynamic properties of colloidal glass and particularly its aging kinetics.

Considering these unique features, we consider in this paper (a) what the differences and similarities are between aging and gelation and (b) how the multicomponent nature of a colloidal Wigner glass affects its aging kinetics.

II. CLASSIFICATION OF DISORDERED STATES OF COLLOIDAL SUSPENSIONS

Before starting the discussion, we define the nonergodic states observed in colloidal suspensions (see Ref. [6] for the details).

A. Attractive gel

We define a gel as a multicomponent fluid, which satisfies the following requirements. (i) At least one of its components is in a disordered nonergodic state. (ii) That component forms an infinite elastic network and thus is percolated mechanically. For the network to be elastic in the observation time scale, the necessary condition is a long-enough lifetime of the junction point, or $E/k_BT \gg 1$ (E being the depth of the attractive potential). (iii) The characteristic length of the network between the two adjacent junctions ξ is much longer than the size of the component. When ξ becomes comparable to the interparticle distance $\bar{l}$, the system should be called "attractive glass" [6] (see below).

B. Attractive and repulsive glass

Including both attractive [21–24] and repulsive glasses, we define a colloidal glass as a colloidal system in a nonergodic disordered state, whose elasticity primarily originates from caging effects. Its mechanical unit has a length scale of the order of the interparticle distance $\bar{l}$ and there is no static inhomogeneity beyond $\bar{l}$. As discussed in Ref. [6], the formation of an attractive glass is possible if E is on the order of k_BT and the particle concentration ϕ is high enough. We stress that even in "attractive glass," repulsive interactions should play the main role in its slow dynamics, although attractive interactions may strongly influence it. This attractive glass state should transform into a gel state at a higher ionic strength (salt concentration) [6].

Here it may be worth pointing out that the boundary between the liquid state and the glassy one is not very easy to determine since its location depends upon how long we wait, for instance, before measuring the viscosity in order to determine whether it is a liquid or a glass.

In the following, we only consider attractive gels and repulsive Wigner glasses, and do not consider the attractive glass for simplicity.

III. DIFFERENCE IN KINETICS BETWEEN GELATION AND AGING OF GLASS

Here we focus our attention on the kinetic aspects of gelation and aging. For gelation due to strong attractive interactions ($E/k_BT \gg 1$), it is well known that a sol state transforms into a gel one at a well-defined gelation point t_{gel} (t denotes time) for which the system is elastically percolated. At t_{gel}, a system exhibits a behavior specific to percolation such as a power-law frequency dependence of the complex modulus, which reflects the percolation transition [25]. For a system where $E/k_BT \sim 1$, however, the gel state cannot be easily distinguished from the sol so clearly and the situation is rather similar to the aging of a glass (see below). In theory, the zero-frequency viscosity also diverges at this point. After this point, the system behaves as an elastic body and the elastic modulus continues to increase. In a phase diagram (see Fig. 2 in Ref. [6]), the gel state can be defined experimentally as the region where t_{gel} becomes finite, or more precisely, on the order of the time scale of experiments. This is similar to the definition of the glassy state. Theoretically, however, the gel state of a thermoreversible gel can be well defined thermodynamically [26]. This is the crucial difference between a reversible gel and a glass.

In contrast to the case of gelation, there is no clear vitrification point for the aging of a glass. Note that viscosity does not diverge at the glass-transition point: it keeps increasing during the aging [9]. This is because there is no physical transition point for vitrification, reflecting its purely kinetic nature. This is a remarkable difference between the two dynamic phenomena, which can be used as a criterion to distinguish them. In the following, we consider this problem in depth.

A. Gelation of sol

1. Stable gel

As mentioned above, the dynamic viscoelastic moduli exhibit a peculiar power-law frequency dependence at the gelation point t_{gel} [25],

$$G'(\omega) \sim G''(\omega) \sim \omega^u, \tag{1}$$

where G' and G'' are the real and imaginary parts of the complex modulus, and ω is the angular frequency. Here the exponent u is related to the fractal dimension d_f of the gel network structure and the spatial dimension D as $u=D/(d_f+2)$. At this gelation point, an infinite percolated network is formed, and thus the static viscosity η diverges. In the time domain, this is observed as a power-law decay. For example, the intensity time correlation function $g_2(t)$ decays as

$$g_2(t) \sim t^{-(1-u)}. \tag{2}$$

This is often used as a signature of the percolation point (see, e.g., [27]). Note that the condition $\xi \gg \bar{l}$ is necessary to obtain the fractal nature and the resulting power-law behavior of the gel. For $t > t_{gel}$, the system becomes nonergodic and $g_2(t)$ does not decay to zero any more in the ideal case.

2. Unstable gels

Here we note that the above behavior of a typical gelation process of a stable gel cannot be applied to gelation of an unstable gel [28] that occurs in an unstable phase-separation region of the phase diagram. Unstable gels may happen at very high salinity, where the electrostatic repulsion is screened so much that the colloids may flocculate. For Laponite, this happens when the electrolyte concentration is larger than 10^{-2} M (see Fig. 2 of Ref. [6]). This is because the structure of an inhomogeneous gel keeps evolving by self-generated internal stress (if it is not strong enough, the gel collapses under its own weight) due to a repetition of the following elementary process: the stress accumulation on the weak strand of the network and the resulting breakup [30]. Thus, the system is not frozen and keeps changing its structure although the process is very slow. Here we note that for unstable gels a very interesting aging behavior, which resembles the aging of Laponite in the glassy state, was observed by Cipelletti *et al.* [28].

3. The case of Laponite suspensions

How do these predictions compare to existing data on Laponite suspensions [29]? The phase diagram of Ref. [6] suggests that at high salt, Laponite is a gel. The power-law frequency dependence of G' and G'' specific to a gelation point was indeed observed with the exponent of $u=0.55$ by Cocard *et al.* [31] for Laponite suspensions of $I \geqslant 10^{-3}$ M. This dynamic feature strongly supports that a nonergodic state of a Laponite suspension of $I \geqslant 10^{-3}$ M is a gel, consistently with the structural features (see Ref. [6]). At this moment, dynamic light scattering measurements during the gelation process at $I \geqslant 10^{-3}$ M are not available. However, we expect that the above-described behavior characteristic of gelation should be observed. This has to be confirmed experimentally in the future.

On the other hand, for low salt, Laponite is a glass [6,9,11]. Experimental studies on the dynamic structure factor $S(q,t)$ at $I=10^{-4}$ M [9] support the glass picture for Laponite suspensions at $I=10^{-4}$ M, since the final decay of the fluctuating parts of the density correlation function is similar for different aging times t_w and does not show the peculiar power-law behavior characteristic to a gelation point t_{gel}. Similar behavior was also observed by Kroon *et al.* [17]. Although this is a subtle problem, the glass picture is supported by (i) the absence of the fractal structure confirmed by light-scattering measurements [10], which indicates the homogeneity of the system over the interparticle distance $\bar{l}$, and (ii) the shape of the phase diagram (see [11] and Fig. 2 of Ref. [6]) and the related discussion for a Laponite suspension of $I \leqslant 10^{-4}$ M (see [6]). On point (i), we note that for a gelation scenario the exponent u should be related to the fractal dimension d_f at a gelation point. Thus, the absence of the q dependence of $S(q)$ [10] cannot be consistent with a scenario that the power-law decay is due to the fractal structure. In addition, Bonn *et al.* [32] show a continuous evolution of u with aging time t_w, with $u \to 0$ when the system becomes nonergodic for $I=10^{-4}$ M.

Osmotic pressure experiments also show that there is a net repulsive interaction between particles [13,33,34]. Moreover, the osmotic pressure decreases with increasing ionic strength. These experimental results are also in qualitative agreement with simulation results and numerical models [35,36]. All these facts support the repulsive glass picture.

Here we briefly discuss the subtlety concerning the state boundary between a gel and a repulsive glass. Since a Laponite particle has a negative surface charge of $Z \sim 10^3$, we cannot apply the linearlized Poisson-Boltzmann theory. Both the far-field form of the potential and the effective interaction are often described using a Debye-Hückel potential with an effective charge Z_{eff} [37–40]. This charge renormalization effectively accounts for the interactions in the inner part of the electric double layer and the effects of the overlapping of double layers. Z_{eff} is determined so that the far-field part of the potential matches the numerical solution of the full nonlinear Poisson-Boltzmann equation. This works rather well for dilute suspensions, where we only need to consider the long-distance behavior of the electrostatic coupling. At finite concentrations of colloids, however, the screened Coulomb form of the potential itself is questionable due to the strong overlap of the condensed and diffuse layers surrounding each particle [37]. The anisotropic shape of Laponite particles makes the situation even worse compared to spherical colloids since we also have to consider the orientational degrees of freedom of particles [41,42]. In this situation, it is quite difficult to theoretically estimate the effective interactions between Laponite particles at finite concentrations. So the boundary between a gel and a repulsive glass may not be very clear theoretically.

Recently, the simultaneous renormalization of the surface charge Z and the screening constant κ have been discussed by Bocquet *et al.* [40] on the basis of the cell approach [39]. They propose that the highly charged colloids can be treated as objects with constant static potential $\sim 4k_BT/e$ (here $e>0$ denotes the elementary charge), independently of shape and physicochemical parameters (size, added 1:1 electrolyte, …). This is based on the physical picture that the electrostatic energy eV_0 of the strongly coupled micro-ions does balance their thermal (entropic) energy k_BT, resulting in a constant effective surface potential for the dressed macro-ion. For Laponite suspensions, the effective charge Z_{eff} was estimated as [41]

$$Z_{eff} = \frac{r_0}{l_B} \frac{2\kappa_{eff}}{1-\exp(-\kappa_{eff} r_0)}, \tag{3}$$

where r_0 is the radius of a disk and l_B is the Bjerrum length given by $l_B = e^2/(\epsilon k_B T)$ (ϵ being the dielectric constant). The effective screening length κ_{eff} (for spherical colloids), on the other hand, is estimated as [42]

$$\kappa_{eff}^4 = \kappa_0^4 + (4\pi l_B Z_{eff}\rho)^2, \quad (4)$$

where κ_0 is the Debye length for an isolated particle in an electrolyte of bulk density n_0 ($\kappa_0^2 = 8\pi l_B n_0$). For $\kappa_{eff} r_0 \sim 1$, Z_{eff} was estimated to be ~ 100 for Laponite suspensions [41].

It is worth stressing here that the effective charge Z_{eff} and the corresponding Debye screening length κ_{eff} should be complex functions of the local ionic strength, the interparticle distances, and the interparticle angles. As will be mentioned later, this fact may play an important role in the aging behavior of Laponite suspensions.

B. Aging of colloidal Wigner glass

Below we discuss possible unique features of the aging of Wigner glass, which crucially differ from those of structural and spin glasses, focusing on the multicomponent features of Laponite suspension.

1. Roles of the ion distribution in colloidal Wigner glass

In a colloidal Wigner glass of Laponite suspension, there may be two important physical factors controlling the aging process: the spatial distribution of colloidal particles $\phi(\boldsymbol{r})$ and that of counterions $\phi_i(\boldsymbol{r})$. The latter, which is an additional degree of freedom that is absent in usual colloidal glasses without charges, controls the strength of electrostatic repulsive interactions, which, in turn, gives the effective volume of particles. Consequently, if there is added salt, the spatial distribution of the salt $\phi_s(\boldsymbol{r})$ is also an additional important factor. For a liquid-glass transition, in general, density (or concentration) is the control parameter. For a colloidal Wigner glass, the effective density (or the effective volume of particle) is a function of not only ϕ, but also ϕ_i and ϕ_s. The aging process of Laponite suspensions may therefore be viewed as finding a quasiglobal minimum in a very complex energy landscape in the multidimensional parameter space of ϕ, ϕ_i, and ϕ_s. The important parameter that controls the range of the electrostatic interactions is the Debye screening length $l_D = \kappa^{-1}$, which is a function of ϕ_i and ϕ_s [6,9,11]. It controls the electrostatic interaction potential between colloids, usually assumed to be given by $\exp(-\kappa r)/r$. The electrical neutrality condition imposes the constraint that $Z\phi - \phi_i = 0$, with Z the charge on the Laponite colloids, $Z \sim 10^3$ e. Thus, the composition fluctuations of the Laponite particles are coupled to those of the small ions. We speculate that the process to establish the ion distribution is very slow because of the additional degrees of freedom such as the translational and orientation degrees of freedom of Laponite particles and their coupling to the degree of the counterion and salt condensation. The local-equilibrium ion distribution around an individual particle should be established very quickly, in a time on the order of $\overline{l^2}/D_i$ (D_i being the diffusion constant of the small ions), which is typically of the order of ms. However, the coupling of the ion distribution to the slow variables can make the establishment of the ion distribution very slow. We will show several pieces of experimental evidence that support this statement below.

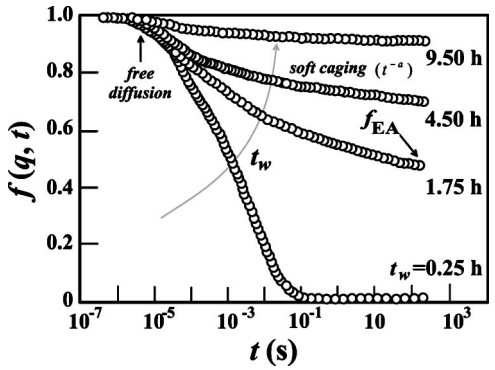

FIG. 1. The temporal change in the decay of $f(q,t)$ for a sample of Laponite concentration 3.5 wt. % and $I = 10^{-4}$ M. Data are taken from Ref. [9]. In the early stage of aging (cage-forming regime), $f(q,t)$ decays in two steps: free diffusion followed by diffusion with weak interparticle interactions. In the late stage of aging (after the formation of cage), a power-law decay likely due to soft caging appears. $f(q,t)$ also starts to have features of a nonergodic state, characterized by the nonzero value of $f(q,\infty)$. To characterize this feature, the value of $f(q,t)$ at the longest observable time (~ 300 s) is defined as the frozen-in component f_{EA}.

2. Unique features of aging in colloidal Wigner glass

For physical gelation, the fraction of the frozen-in component, which is called the Debye-Waller factor or the Edwards-Anderson order parameter [43], should increase with time, reflecting the development of the network structure. This is because more elastic components are involved in the percolated network as the gelation proceeds. For usual glasses, it is predicted by the aging theory based on a droplet picture of spin glass [43,44] that the fraction of the frozen-in component (or the fraction of the α relaxation) relative to fast β relaxation should be constant with time for the late stages of aging. This was also confirmed by numerical simulations [45]. In our previous experiments, we found that the frozen-in component, or the Edwards-Anderson order parameter, increases with time, contrary to what happens in the spin-glass theory of aging [43,44]. Apparently, this fact seems more natural if we consider the nonergodic state of Laponite suspensions as a gel rather than a glass. However, we argue here that for the colloidal Wigner glass, the Edwards-Anderson order parameter should increase with time, reflecting the increase in the strength of the repulsive interaction due to the reorganization of the distribution of particles, counterions, and salt ions, and the resulting change in the degree of the ion localization on the surface of Laponite particles. The physical picture is that the effective volume per particle increases and thus the particles are more strongly confined as the aging proceeds. This is markedly different from the droplet picture of spin glass [43–45], where the magnetization is constant with time but only the dynamic coherence length increases with time.

Here we check the relevance of this picture in more detail. The density-density correlation function $f(q,t)$ decays in time. The way of its decay changes with the aging time, as illustrated in Fig. 1. In the early stage of aging, $f(q,t)$ decays in two steps: initial free diffusion and particle diffusion under

weak interparticle interactions. The former is described by an exponential decay, while the latter is described by the stretched exponential one [46]. We identify this regime of aging as the "cage-forming regime." We believe that in this regime, a distinct cage that can trap a particle for a certain period of time is not yet formed. In the late stages of aging, on the other hand, $f(q,t)$ decays in three steps: (i) a free-diffusion regime [9,17,47], which is characterized by a single exponential decay, (ii) a soft-caging regime, which exhibits the power-law-like decay [17,47], and (iii) a regime of escaping from the cage, which is characterized by the stretched exponential decay [9,17,47]. There is no clear plateau region that separates rattling motion within the cage from cage escape dynamics. Instead, $f(q,t)$ decays very slowly in regime (ii), obeying a power-law dynamics.

A power-law decay following the fast β process is predicted by the mode-coupling theory (MCT) [48] and is known as the cage process wing: $f(q,t)=f_{\mathrm{EA}}+A(t/\tau_\beta)^{-a}$, where A is a constant and τ_β is the characteristic time of the fast β process. In the MCT scenario, this process is further followed by the power law of $f_{\mathrm{EA}}-B(t/\tau_\beta)^b$, where B is a constant and b is related to a. This peculiar process is known as the von Schweidler law [48].

However, we point out that the power-law behavior observed in Laponite suspensions is crucially different from this schematic MCT scenario: In Laponite suspensions, the time span of the power-law regime increases with time and reaches over five decades in time. This feature cannot be explained by the MCT scenario. Even for hard-sphere colloidal glasses, for which MCT is known to work well [49], the time span of the power-law regime is two to three decades at most [50]. We speculate that such a pronounced existence of regime (ii) may reflect the soft nature of long-range Coulomb interactions. The above aging behavior is quite unique and specific to the aging of a colloidal Wigner glass and reflects the increase in the effective volume fraction of colloidal particles ϕ_{eff} with aging. The relevance of this picture is supported by the fact that the change in the decay pattern of Fig. 1 closely resembles that induced by the increase of the volume fraction of hard-sphere colloids reported by van Megen and Underwood (see Figs. 5 and 13 in Ref. [50]). That is, the effective volume of Laponite ϕ_{eff} increases with the aging time.

In relation to this, it is worth mentioning that the lack of a completely flat plateau has been observed also in simulations of aging of attractive glasses and has been attributed to the finite lifetime of bonds [51]. This similarity in the aging behavior between repulsive and attractive glass may stem from the common origin that the cage is too soft to trap particles.

The cage is consequently soft in the intermediate stage of aging, but it becomes harder with increasing the aging time, reflecting the increase in ϕ_{eff}. This change in the nature of the cage is supported by the following pieces of experimental evidence.

We identify the late-time value of $f(q,t)$ as the Edwards-Anderson order parameter f_{EA} (see Fig. 1). It is initially zero and slowly increases with aging [9,17]. We previously estimated [9] the cage size $\bar{\delta}=\sqrt{\langle\delta^2\rangle}$, where $\langle\delta^2\rangle$ is the mean-square displacement of particles, from the Edwards-Anderson order parameter $f(q,\infty)$ by using a model that describes the motion of Brownian particles trapped in a harmonic potential [52]. In this simple model, $f(q,\infty)=\exp(-q^2\langle\delta^2\rangle)$. This is exactly the definition of the Debye-Waller factor for glassy systems [5]. The cage size $\bar{\delta}$ can then be estimated from the q dependence of $f(q,\infty)$. According to our study on glassy Laponite suspensions ($\phi=3.5$ wt. %, $I=10^{-4}$ M), $\bar{\delta}$ is about 80 nm when $t_w\sim 0$, but it monotonically decreases with t_w and approaches 17 nm with $t_w\to\infty$ (see Fig. 2). It becomes almost constant for $t_w>5000$ s. This clearly shows the increase in the repulsive interactions with increasing t_w.

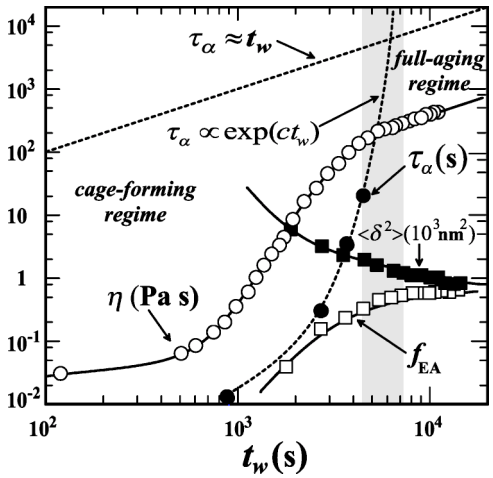

FIG. 2. Temporal change in η, f_{EA}, δ^2, and τ_α as a function of t_w, which was observed during the aging of a Laponite suspension ($\phi=3.5$ wt. % and $I=10^{-4}$ M) [9]. It is clear that the full aging behavior ($\tau_\alpha\sim t_w$) is observed only after the cage is formed. The shaded region is the crossover region from the cage-forming to the full-aging regime. Before this crossover, f_{EA} and $\langle\delta^2\rangle$ are strongly changing with time, reflecting the evolution of soft cage.

We also found that the total scattering intensity S is decreasing in time (see Fig. 6 in Ref. [6] and the related discussion there), becoming roughly constant for $t_w>5000$ s. Such a decrease in the scattering intensity was confirmed for the scattering angle of 30°–90° and also by the decrease of the turbidity. Consistently with the temporal change in $\bar{\delta}$, this behavior can also be explained by a decrease in the susceptibility (the increase in the osmotic compressibility), or equivalently the increase in the repulsive interactions with t_w. Similar behavior of the decay of the scattering intensity during aging (at $q=2.3\times10^5$ cm^{-1}) was also reported by Knaebel *et al.* [12]. All these facts support our physical picture. The time regime before $t_w<5000$ s is the cage-forming regime, while that after $t_w>5000$ s is the full-aging regime, where f_{EA} reaches more than 50% of its final value at $t_w\to\infty$. Such a temporal decrease in the scattering intensity might occur if small bubbles or small aggregates slowly dissolve during the aging. However, the absence of the corresponding diffusive modes is against such a possibility. Furthermore, the fact that the time span of the decay of the scattering intensity corresponds to the cage-forming regime seems to be more than an accidental coincidence.

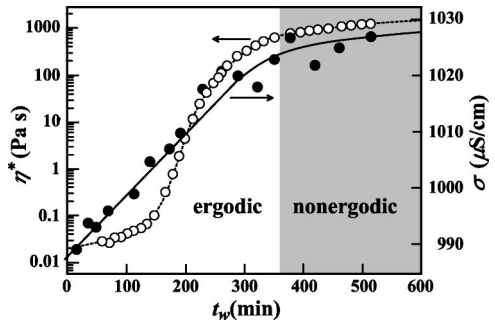

FIG. 3. Temporal change in the conductivity σ and the complex viscosity η^* measured at the frequency of 0.05 Hz during the aging. The Laponite concentration was 3.2 wt. % and the pH was 10. σ increases almost linearly with t_w in the early stage, where the system is ergodic in the dynamic light scattering experiment, while it tends to saturate in the late stage. This crossover gradually occurs around the transition between the cage-forming (ergodic) and the full-aging (nonergodic) regime.

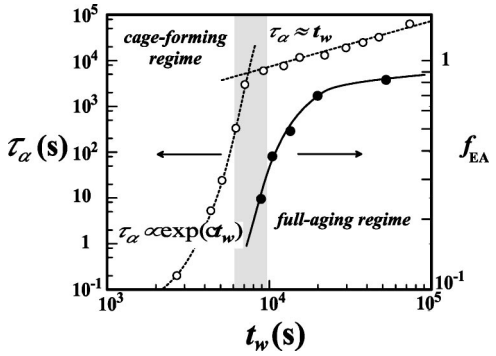

FIG. 4. Temporal change in f_{EA} and τ_α as a function of t_w, which was observed for a Laponite solution ($\phi=1.36$ wt. % and $I=10^{-4}$ M). Data were taken from Ref. [47]. When f_{EA} approaches the final value, the aging behavior transforms (in the shaded crossover region) from the cage-forming regime, where τ_α increases exponentially with t_w, to the full-aging regime, where $\tau_\alpha \sim t_w$.

For the case of gelation, the scattering intensity should increase with the aging time, reflecting the growth of a fractal network (see Fig. 6 in [6]).

To show that the electrostatic interaction changes, we show here the results of our conductivity measurements during the aging. It is found that the conductivity σ increases almost linearly with the aging time in the ergodic regime, but tends to saturate in the nonergodic regime (see Fig. 3). In this ergodic regime, the structural relaxation time τ_α grows exponentially, as in other cases. The temporal increase in σ should reflect the decrease in the number of the strongly bound counterions, which are immobilized in the Stern layer, with increasing the aging time. The initial conductivity σ_{ini} (990 μS/cm) should include the contribution of OH ions σ_{OH} and that of the counterions (Na^+) released from Laponite particles, σ_{Na}. Since $\sigma_{\mathrm{OH}} \sim 20$ μS/cm, we obtain $\sigma_{\mathrm{Na}} \cong 970$ μS/cm. Thus, the number density of Na^+ ions n is estimated as $n \sim 19.5$ mM, from $n=\sigma_{\mathrm{Na}}/\mu_{\mathrm{Na}}e$, where μ_{Na} is the mobility of Na^+ ion ($\mu_{\mathrm{Na}}=5.19\times10^{-8}$ m^2 s^{-1} V^{-1}) and e is the electron charge. Since the number density of Laponite particles in 3.2 wt. % solution is $N=29.2$ μM, the number of Na^+ ions released from each Laponite particle is estimated to be 660, which is in agreement with the number of the negative charge per particle surface reported in the literature, 10^3 e^-. From the amount of the change in the conductivity ($\Delta\sigma \sim 35$ μS/cm), we can also estimate the increase in the unbound Na^+ ions during the aging as $\Delta n=\Delta\sigma/\mu_{\mathrm{Na}}e \sim 0.7$ mM. This increase of 0.7 mM should have a considerable effect on noting that the ionic strength of the system is 0.1 mM.

From the above, we can estimate Z_{eff} at $t_w=0$ min and 500 min, respectively, as 660 and 690. These values are much higher than the theoretically estimated saturation value of Z for Laponite suspensions ($Z \sim 100$) [41] (see Sec. III A 3). It is also known from experimental studies on spherical colloids that the effective charge estimated from a Debye-Hückel-type pair interaction potential is systematically smaller than that estimated from the conductivity by some 40% [53]. Thus it is not easy to estimate Z_{eff} and κ_{eff} from our conductivity data in a direct manner. What we can conclude from our measurements is that both Z_{eff} and κ_{eff} increase with the aging before the ergodicity breaking. These changes bring two antagonistic effects on the effective Coulomb interactions between Laponite particles: the range of interaction decreases due to stronger screening, while the amplitude increases due to the increase in the effective charge. We note that which effects become more dominant also depends crucially upon the particle concentrations. Although we cannot draw any definitive conclusion, the scattering intensity indicates that the interparticle interactions become more repulsive with aging, also in agreement with the observation that the position fluctuations in the cage $\langle \delta^2 \rangle$ decreases during the aging.

Now we discuss the temporal change of τ_α. τ_α increases exponentially with t_w [46,47,54] until τ_α becomes comparable to t_w (see Figs. 2, 4, and 5),

$$\tau_\alpha \sim \exp(ct_w), \tag{5}$$

where c is a constant, and subsequently evolves linearly with t_w [12,47] (see Figs. 2, 4, and 5),

$$\tau_\alpha \sim t_w. \tag{6}$$

The latter corresponds to the so-called full-aging regime [44]. This crossover is natural in the sense that τ_α cannot exceed t_w. The fact that the aging part of the response function scales as t/t_w means that the effective relaxation time of a system in the glass region is set by its age t_w. This further means that the microscopic time scale is no longer relevant to the aging dynamics for asymptotically long aging times.

On the basis of these experimental findings, we propose that the observed aging process of a colloidal Wigner glass can be divided into two regimes (see Figs. 2, 4, and 5). In the early stage of aging, the effective volume fraction increases with time, reflecting the increase in the repulsive interaction between particles. In this early stage, the Debye-Waller factor (f_{EA}) increases with time and the scattering intensity (S) decreases. We also note that in this early stage, τ_α increases steeply with t_w (see below and Figs. 2, 4, and 5), reflecting

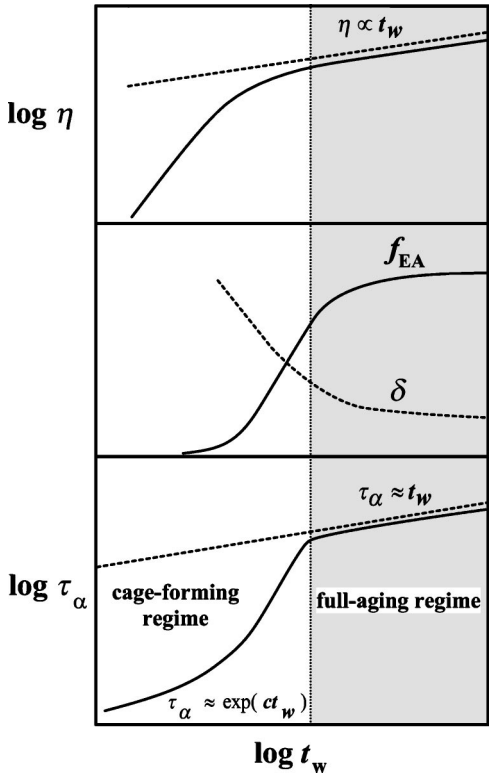

FIG. 5. Schematic figure representing the temporal change in η, f_{EA}, δ, and τ_α as a function of t_w. We propose that the full-aging behavior ($\tau_\alpha \sim t_w$) is observed only when particle rearrangements are the only kinetic process. Before the full aging, f_{EA} and δ are strongly changing with time, reflecting the evolution of the soft cage. Accordingly, there is no proportionality between η and τ_α.

the gradual transformation from a liquid state to a glassy one due to the slow increase in the repulsive interactions with aging. Thus, we call this early stage of aging the "cage-forming regime." The system subsequently enters into the late stage, where the "droplet picture of spin glasses" [43–45] works properly and thus the proposed scaling relations hold for this regime. We call this late stage the "full-aging regime." The existence of the cage-forming regime is therefore a characteristic feature of the colloidal Wigner glass. The two stages can be clearly separated by looking at the behavior of δ. In the early stage, δ decreases with t_w, while in the late stage it becomes constant (see Figs. 2, 4, and 5).

This type of two-stage aging is not observed for usual glass-forming liquids such as polymers. In glass-forming polymers, for example, the initial stage of the aging is well described by the full aging ($\tau_\alpha \propto t_w$) [55]. This may be due to the fact that there already exist well-developed cages even in a liquid state for a usual glass-forming liquid. In addition, we note that there is no change in the interaction potential for such liquids and thus the amount of the density change required for inducing a liquid-glass transition is generally very small.

Finally, we note that the apparently quite similar two-stage aging behavior was observed for unstable colloidal gels [28,56]. We speculate that this two-stage aging reflects the similar crossover behavior from the cluster-growth regime to the gel-aging regime. For example, the first stage is the process of the growth of clusters. The growing clusters either fill up the space or percolate with each other, which may lead to the nonergodic full-aging regime.

In relation to this, we suggest that there should be a one-to-one correspondence between the crossover from the cage-forming to the full-aging regime and the ergodic-to-nonergodic transition. The exponential growth of τ_α may be unique to the cage-forming ergodic regime, while the full-aging behavior ($\tau_\alpha \sim t_w$) may be to the nonergodic glassy regime. Our experimental results are basically consistent with this scenario. The above-mentioned behavior in unstable colloidal gels also seems to be consistent with it, on noting that a system becomes nonergodic after the growing clusters of aggregates either fill up the space or percolate with each other. Furthermore, aging experiments in ordinary glasses are usually performed below the glass-transition temperature T_g, where a system is in the nonergodic glassy state. Thus, the absence of the cage-forming regime in such experiments is quite natural. The cause for the exponential growth of the time scale in the ergodic cage-forming regime remains a theoretical problem for future investigation.

3. Two-stage aging kinetics

We now consider a simple model, based on the experimental observations, for the relation between the viscosity and the relaxation time. We express the two-stage aging process in terms of the average barrier for particle motion. The structural relaxation time is often expressed by using the average barrier height U for particle motion as

$$\tau_\alpha = \tau_0 \exp(U/k_B T), \tag{7}$$

where τ_0 is the inverse of a typical attempt frequency. During the aging, U is a function of the aging time t_w and we express it as $U(t_w) = U_0 + \Delta U(t_w)$, where U_0 is U at $t_w = 0$. The experiments at early times, i.e., Eq. (5), indicate that ΔU grows linearly with t_w as

$$U(t_w) = U_0 + ck_B T t_w. \tag{8}$$

On the other hand, for late times (full aging), Eq. (6) indicates that ΔU grows logarithmically with t_w as

$$U(t_w) = U_0 + k_B T \ln\left(1 + \frac{t_w}{\tau_0}\right). \tag{9}$$

At very late times, ΔU may become constant and approach ΔU_f. The change in the barrier height is schematically shown in Fig. 6.

This barrier height may be related to the domain size in the droplet picture [43]: The linear growth of ΔU means the power-law growth of the domain size (coherence length) R, while its logarithmic growth means the logarithmically slow growth of R. The reason for the initial linear growth of $U(t_w)$ for the Wigner glass is not clear at this moment.

4. Relation between the viscosity η and the structural relaxation time τ_α

Next we consider the relationship between the viscosity η and the structural relaxation time τ_α, focusing on the above

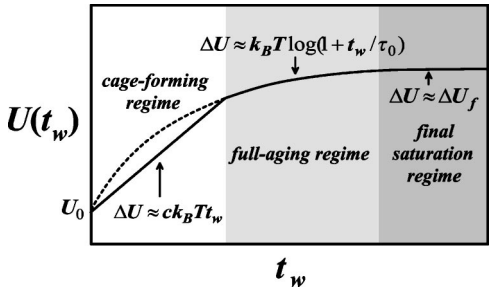

FIG. 6. Schematic figure representing the temporal change in the effective barrier height U as a function of t_w. Note that $\tau_\alpha(t_w)$ cannot exceed t_w. Thus, the initial fast linear growth is switched into the slower logarithmic one, and then further into the final equilibrium one. This last saturation behavior is observed in the aging of glass-forming polymers [55].

crossover behavior. The simplest constitutive equation of viscoelastic matter is given by a Maxwell equation,

$$\frac{\partial \sigma}{\partial t} = -\frac{\sigma}{\tau_\alpha} + M\dot{\gamma}, \tag{10}$$

where σ is the mechanical stress, $\dot{\gamma}$ is the strain (shear) rate, τ_α is the structural relaxation time, and M is the elasticity. M should be proportional to the nonergodicity parameter, or the Edwards-Anderson parameter, f_{EA}, for any glass-forming system. This is based on a simple but natural idea that the solid nature, or the static elasticity, of any system should be described solely by its nonergodicity parameter, which tells us how solidlike a system is. Note that for a glass-forming liquid, its solidlike elastic nature stems solely from *caging* effects. For ordinary glass-forming systems, it is known that f_{EA} is almost independent of temperature above the so-called mode coupling T_c and below T_c it only slightly increases toward 1 upon cooling. This is due to the fact that the change of density as a function of temperature is very small for ordinary liquids, although this small change does lead to a drastic slowing down of the dynamics near the liquid-glass transition. In other words, the density of an ordinary liquid is already high enough to produce the so-called caging effects. For the colloidal Wigner glass, on the other hand, f_{EA} slowly increases from zero to a finite value during the aging (see Fig. 7), likely reflecting the increase of the effective volume fraction with aging.

If we assume a quasisteady state during the aging in Eq. (10), we have $\eta(t_w)=M(t_w)\tau_\alpha(t_w)$. As mentioned above, it is reasonable to assume that $M(t_w)=kf_{\mathrm{EA}}(t_w)$, where k is a constant. Thus, the plateau modulus $G_p'(\omega,t_w)=M(t_w)$ should be proportional to the nonergodicity parameter $f_{\mathrm{EA}}(t_w)$. This consideration leads to a conclusion that $\eta(t_w) \sim \tau_\alpha(t_w)f_{\mathrm{EA}}(t_w)$. Thus, the increase in η with aging originates from the following two factors: (i) the increase in τ_α with aging [9,12,46,47] and (ii) the increase in the nonergodicity parameter f_{EA} with aging [9,17]. As shown in Fig. 7, this relation explains the temporal change of the magnitude of the complex viscosity η^* quite well. Note that $\eta^* = \sqrt{G'^2+G''^2}/\omega = M\tau_\alpha/\sqrt{1+\omega^2\tau_\alpha^2}$. Thus, the quasiequilibrium

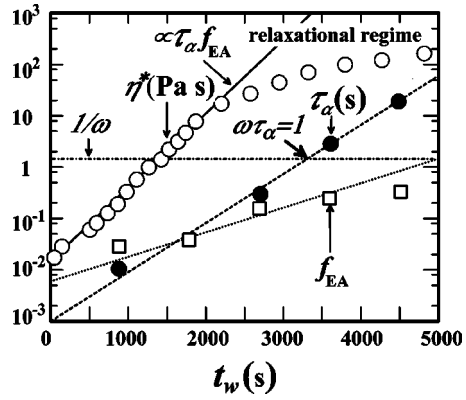

FIG. 7. Relation among η^*, τ_α, and f_{EA}. Data are taken from Ref. [9], and are the same as those of Fig. 2. The relation $\eta^* \propto \tau_\alpha f_{\mathrm{EA}}$ is observed to hold well. Note that in the early stage of aging, $\eta^* \cong 0.015\exp(0.0033t_w) \cong 2500\tau_\alpha\ f_{\mathrm{EA}}$ Pa s (solid line), $\tau_\alpha \cong 0.001\exp(0.0022t_w)$ s (dashed line), and $f_{\mathrm{EA}} \cong 0.006\exp(0.0011t_w)$ (dotted line). The deviation of η^* from the solid line for $t_w > 2000$ s is due to the dynamic crossover between the characteristic time of mechanical perturbation $(1/\omega)$ and τ_α, which occurs around $\omega\tau_\alpha=1$. In this experiment, the measurement frequency f was 0.1 Hz (note that $\omega=2\pi f$).

assumption is violated when τ_α approaches the characteristic observation time $1/\omega$ (in our experiment [9] the measurement frequency f was set to 0.1 Hz).

In the very early stage of aging, f_{EA} is almost zero and the condition $\omega\tau_\alpha \gg 1$ is not satisfied for typical frequencies of the rheological experiment. Then, the above relation may not hold. This may be the case for the data reported by Abou *et al.* (see Fig. 8 of [46]), where η^* grows much faster than τ_α especially in the early stage.

IV. SUMMARY

In summary, we have discussed the differences and the similarities in the kinetics between aging and gelation. We also point out the unique features of the aging of colloidal Wigner glass, which are crucially different from those of the aging of spin and structural glasses. The aging of Wigner glass may be divided into three regimes: (i) a cage-forming regime, (ii) a full-aging regime, and (iii) a final saturation regime. The final regime has not been observed experimentally for the Wigner glass, but was observed for glass-forming polymers [55]. The relevance of the two-step aging scenario [i.e., the existence of regime (i) and (ii)] has been confirmed by the analysis of the experimental data.

We have discussed the possibility of the slow temporal change in the interparticle electrostatic interactions in the cage-forming regime. This scenario is supported by our conductivity measurements. Due to the complex nature and effect of charge renormalization, however, it is quite difficult to infer the change in the interparticle interactions from that in the conductivity. The temporal increase in the osmotic compressibility, which is deduced from the change in the light scattering intensity, seems to support the increase in the repulsive interactions during the aging, but the validity of this conclusion should be checked more carefully. Further

theoretical studies on the electrostatic interactions in highly charged colloids at finite concentrations are also highly desirable.

We have to note that there still remain many unanswered questions such as why τ_α grows exponentially with the aging time for short aging times and what is the physics behind the striking similarity of the aging behaviors between the colloidal Wigner glass and aggregating colloids despite the apparent difference in the physical process between the two. We propose that there should be a one-to-one correspondence between the crossover from the cage-forming to the full-aging regime and the ergodic-to-nonergodic transition. On noting that both colloidal Wigner glasses and aggregating colloids accompany the ergodic-to-nonergodic transition during the aging, our picture suggests that the similarity can be a consequence of the universal features of the ergodic-to-nonergodic transition of a system whose initial state is gas-like in the sense that there are few caging effects on particle motion. Further experimental and theoretical studies are highly desirable to elucidate the differences and the similarities between glasses and gels. The understanding of the aging in attractive glass also remains a problem for future investigations. Ultimately, this will provide useful information for the possibility of finding a universal physical description of nonergodic (jammed) states [1–3] including glasses and gels.

ACKNOWLEDGMENTS

LPS de l'ENS is UMR8550 of the CNRS, associated with the universities Paris 6 and Paris 7. H.T. is grateful to Ecole Normale Supérieure (ENS) for financial assistance and for the kind support during his stay at ENS, during which time a part of this work was carried out. He also appreciates financial support from the Ministry of Education, Culture, Sports, Science and Technology, Japan.

[1] A. J. Liu and S. R. Nagel, Nature (London) **396**, 21 (1998).
[2] V. Trappe, V. Prasad, L. Cipelletti, P. N. Serge, and D. A. Weitz, Nature (London) **411**, 772 (2001).
[3] L. Cipelletti and L. Ramos, Curr. Opin. Colloid Interface Sci. **7**, 228 (2002).
[4] P. G. de Gennes, *Scaling Concepts in Polymer Physics* (Cornell University Press, Ithaca, NY, 1979).
[5] E. Donth, *The Glass Transition* (Springer-Verlag, Berlin, 2001).
[6] H. Tanaka, J. Meunier, and D. Bonn, Phys. Rev. E **69**, 031404 (2004).
[7] S. Z. Ren and C. M. Sorensen, Phys. Rev. Lett. **70**, 1727 (1993).
[8] Laponite is a synthetic clay colloid with a disk shape; its diameter is ~30 nm, its thickness is ~1 nm, and the number of surface charges on a face is the order of 10^3 e.
[9] D. Bonn, H. Tanaka, G. Wegdam, H. Kellay, and J. Meunier, Europhys. Lett. **45**, 52 (1998).
[10] D. Bonn, H. Kelly, H. Tanaka, G. Wegdam, and J. Meunier, Langmuir **15**, 7534 (1999).
[11] R. Levitz, E. Lecolier, A. Mourchid, A. Delville, and S. Lyonnard, Europhys. Lett. **49**, 672 (2000).
[12] A. Knaebel, M. Bellour, J.-P. Munch, V. Viasnoff, F. Lequeux, and J. L. Harden, Europhys. Lett. **52**, 73 (2000).
[13] A. Mourchid, A. Delville, J. Lambard, E. Lécolier, and P. Levitz, Langmuir **11**, 1942 (1995); A. Mourchid, A. Delville, and P. Levitz, Faraday Discuss. **101**, 275 (1995).
[14] F. Pignon, J.-M. Piau, and A. Magnin, Phys. Rev. Lett. **76**, 4857 (1996).
[15] F. Pignon, A. Magnin, and J.-M. Piau, Phys. Rev. Lett. **79**, 4689 (1997).
[16] F. Pignon, A. Magnin, J.-M. Piau, B. Cabane, P. Lindner, and O. Diat, Phys. Rev. E **56**, 3281 (1997).
[17] M. Kroon, G. H. Wegdam, and R. Sprik, Phys. Rev. E **54**, 6541 (1996).
[18] M. Kroon, W. L. Vos, and G. H. Wegdam, Phys. Rev. E **57**, 1962 (1998).
[19] R. G. Avery and J. D. F. Ramsay, J. Colloid Interface Sci. **109**, 448 (1986).
[20] T. Nicolai and S. Cocard, Langmuir **16**, 8189 (2000); Eur. Phys. J. E **5**, 221 (2001).
[21] T. Eckert and E. Bartsch, Phys. Rev. Lett. **89**, 125701 (2002).
[22] K. N. Pham, A. M. Puertas, J. Bergenholtz, S. U. Egelhaaf, A. Moussaïd, P. N. Pusey, A. B. Schofield, M. E. Cates, M. Fuchs, and W. C. K. Poon, Science **296**, 104 (2002).
[23] F. Sciortino, Nat. Mater. **1**, 145 (2002).
[24] K. A. Dawson, Curr. Opin. Colloid Interface Sci. **7**, 218 (2002).
[25] H. H. Winter and F. Chambon, J. Rheol. **30**, 357 (1986); H. H. Winter and M. Mours, Adv. Polym. Sci. **134**, 167 (1997).
[26] F. Tanaka and A. Matsuyama, Phys. Rev. Lett. **62**, 2759 (1989).
[27] J. E. Martin, J. Wilcoxon, and J. Odinek, Phys. Rev. A **43**, 858 (1991).
[28] L. Cipelletti, S. Manley, R. C. Ball, and D. A. Weitz, Phys. Rev. Lett. **84**, 2275 (2000).
[29] Here we consider only Laponite suspensions prepared at pH 10, since it is known that maintaining Laponite at a pH above 9 prevents dissolution of the particles and helps the reduction of the positive charges on the rim of the particle.
[30] H. Tanaka, Phys. Rev. E **59**, 6842 (1999); J. Phys.: Condens. Matter **12**, R207 (2000).
[31] S. Cocard, J. Francois, and T. Nicolai, J. Rheol. **44**, 585 (2000).
[32] D. Bonn, P. Coussot, H. T. Huynh, F. Bertrand, and G. Debrégeas, Europhys. Lett. **59**, 786 (2002).
[33] A. Mourchid, E. Lécolier, H. Van Damme, and P. Levitz, Langmuir **14**, 4718 (1998).
[34] S. Bhatia, J. Barker, and A. Mourchid, Langmuir **19**, 532 (2003).
[35] R. J. F. Leote de Carvalho, E. Trizac, and J. P. Hansen, Europhys. Lett. **43**, 368 (1998); Phys. Rev. E **61**, 1634 (2000).
[36] L. Harnau, D. Costa, and J. P. Hansen, Europhys. Lett. **53**, 729 (2001).

[37] L. Belloni, Colloids Surf., A **140**, 227 (1998).
[38] H. Ohshima, T. Healy, and L. R. White, J. Colloid Interface Sci. **90**, 17 (1982).
[39] S. Alexander, P. M. Chaikin, P. Grant, G. J. Morales, and P. Pincus, J. Chem. Phys. **80**, 5776 (1984).
[40] L. Bocquet, E. Trizac, and M. Aubouy, J. Chem. Phys. **117**, 8138 (2002).
[41] E. Trizac, L. Bocquet, R. Agra, J.-J. Weis, and M. Aubouy, J. Phys.: Condens. Matter **14**, 9339 (2002).
[42] E. Trizac, M. Aubouy, and L. Bocquet, J. Phys.: Condens. Matter **15**, S291 (2003).
[43] J.-P. Bouchaud, L. F. Cugliandolo, J. Kurchan, and M. Mezard, in *Spin Glasses and Random Fields*, Directions in Condensed Matter Physics Vol. 12, edited by A. P. Young (World Scientific, London, 1998).
[44] J.-P. Bouchaud, in *Soft and Fragile Matter*, edited by M. E. Cates and M. R. Evans (IOP Publishing, London, 2000).
[45] W. Kob, in *Soft and Fragile Matter*, edited by M. E. Cates and M. R. Evans (IOP Publishing, London, 2000).
[46] B. Abou, D. Bonn, and J. Meunier, Phys. Rev. E **64**, 021510 (2001).
[47] M. Bellour, A. Knaebel, J. L. Harden, F. Lequeux, and J.-P. Munch, Phys. Rev. E **67**, 031405 (2003).
[48] W. Götze and L. Sjögren, Rep. Prog. Phys. **55**, 241 (1992).
[49] S. K. Lai, W. J. Ma, W. van Megen, and I. K. Snook, Phys. Rev. E **56**, 766 (1997).
[50] W. van Megen and S. M. Underwood, Phys. Rev. E **49**, 4206 (1994).
[51] E. Zaccarelli, G. Foffi, F. Sciortino, and P. Tartaglia, Phys. Rev. Lett. **91**, 108301 (2003); G. Foffi, E. Zaccarelli, S. Buldyrev, F. Sciortino, and P. Tartaglia, J. Chem. Phys. **120**, 8824 (2004).
[52] B. Bern and R. Pecora, *Dynamic Light Scattering* (Wiley, New York, 1976); P. N. Pusey and W. van Megen, Physica A **157**, 705 (1989); J. G. H. Joosten, E. T. F. Geladé, and P. N. Pusey, Phys. Rev. A **42**, 2161 (1990); J.-Z. Xue, D. J. Pine, S. T. Milner, X.-l. Wu, and P. M. Chaikin, *ibid.* **46**, 6550 (1992).
[53] P. Wette, H. J. Schöpe, and T. Palberg, J. Chem. Phys. **116**, 10 981 (2002).
[54] C. Wilhelm, F. Elias, J. Browaeys, A. Ponton, and J.-C. Bacri, Phys. Rev. E **66**, 021502 (2002).
[55] P. A. O'Connell and G. B. McKenna, J. Chem. Phys. **110**, 11 057 (1999).
[56] R. J. M. d'Arjuzon, W. Frith, and J. R. Melrose, Phys. Rev. E **67**, 061404 (2003).